

# Persistent current formation in a high-temperature Bose-Einstein condensate: an experimental test for c-field theory

S. J. Rooney,<sup>1</sup> T. W. Neely,<sup>2,\*</sup> B. P. Anderson,<sup>2</sup> and A. S. Bradley<sup>1</sup>

<sup>1</sup>*Jack Dodd Center for Quantum Technology, Department of Physics, University of Otago, Dunedin 9016, New Zealand.*

<sup>2</sup>*College of Optical Sciences, University of Arizona, Tucson, Arizona 85721, USA.*

(Dated: August 23, 2012)

We quantitatively model a stirred Bose-Einstein condensate at high temperature using grand-canonical c-field theory, comparing simulations with available experimental data. Stirring generates a chaotic array of quantum vortices that decays, via thermal damping and noise, to form a macroscopic persistent current in a toroidal confining potential. We perform 3D numerical simulations of the full dynamical evolution of the system within the truncated-Wigner representation using a consistent energy cutoff and a priori determined reservoir parameters. This work gives the first quantitative comparison of theory with experiment for dissipative vortex dynamics in a trapped Bose-Einstein condensate from first principles, with no fitted parameters. We find that both damping and noise are required to give a quantitative account of the dynamics, and that the size of the persistent current and timescale of its formation are in close agreement with experimental data. In contrast, comparison of experimental data with damped Gross-Pitaevskii theory excludes it as a quantitative model of high temperature vortex dynamics.

PACS numbers: 67.85.De, 03.75.Lm, 03.75.Kk, 67.85.Hj

As highly controllable degenerate matter wave systems, dilute Bose gases offer a unique window into the realm of many body quantum mechanics [1]. Yet developing a quantitative non-equilibrium description of high-temperature Bose gases poses a major theoretical challenge [2, 3], particularly near the critical temperature where the breakdown of mean field theory renders two-fluid theories [4] inoperative. Exact methods offer insight for small systems [5], but for large hot systems, that typically occur near the critical point of evaporative cooling, quantitative tests of theory have been confined to equilibrium critical fluctuations [6], and collective modes [7]. As conspicuous experimental signatures of superfluid motion with long lifetimes [8], quantum vortices offer a different test for non-equilibrium theory.

Since the first observations of quantized vortices in dilute gas Bose-Einstein condensates (BEC) [9], experimental studies of their properties have proliferated [10]. Vortex motion is highly sensitive to thermal fluctuations and nonlinear interactions between vortices and other excitations in the fluid [11]. Many experiments depend on the presence [12] or formation [13] of a rotating thermal reservoir to take the superfluid from a non-rotating state to one containing vortices. Dissipative vortex dynamics in harmonically trapped BECs have been treated within Zaremba-Nikuni-Griffin (ZNG) theory at low temperatures [14], and the Stochastic Projected Gross-Pitaevskii equation (SPGPE) [15] at high temperatures [8, 16], but the predictions for vortex lifetimes have yet to be tested experimentally. In an annular trapping geometry, such as may be created using an obstacle potential in a harmonic trap [17], a vortex can be freely moving in the bulk superfluid, or pinned to the obstacle, forming a stable persistent current. Persistent currents have previously been created in BECs through coher-

ent optical manipulation [18], and the Kibble Zurek mechanism [17]. Despite the importance of quantized vortices in in dissipative superfluid phenomena and in the formation and stability of persistent currents, their motion at high temperature is largely untested.

In this article we present a study of persistent current formation via dissipative vortex dynamics in the presence of a large thermal reservoir. We perform large scale numerical simulations of an experimental forcing sequence [19] using the SPGPE to provide the first quantitative test of theory of vortex dynamics at high temperature, with no fitted parameters. We also compare the SPGPE with the damped GPE (dGPE) [20] which is obtained by setting the noise in the SPGPE to zero, and has been a useful tool for understanding vortex motion [21, 22].

The SPGPE is a grand-canonical c-field method formulated from a microscopic derivation of reservoir interactions in the Wigner phase-space representation [15, 23], and is valid right through the phase transition [3]. The equation of motion bears a superficial resemblance to the GPE, but also contains damping and noise terms arising from the reservoir interaction, and evolves both the condensed and non-condensed fractions of the system lying below a specified energy cutoff. The cutoff is a central formal and technical aspect of the theory. It allows the formally divergent continuum SGPE theory to be consistently extended beyond one spatial dimension [15]. In this work we use the simple-growth SPGPE [24], which neglects reservoir interactions involving number-conserving scattering between c-field and thermal reservoir atoms. These processes are known to be weak in quasi-equilibrium situations [3]. In a simple-growth SPGPE study of vortices occurring spontaneously during the phase-transition [17] a single fitted parameter (the reservoir coupling strength) was used to give vortex formation data in close agreement with the experiment. However, in near-equilibrium situations the reservoir interaction parameters can be determined *a-priori* [8, 24], allowing the SPGPE to perform quantitatively accurate calculations of dis-

\* Current address: School of Mathematics and Physics, University of Queensland, QLD 4072, Australia.

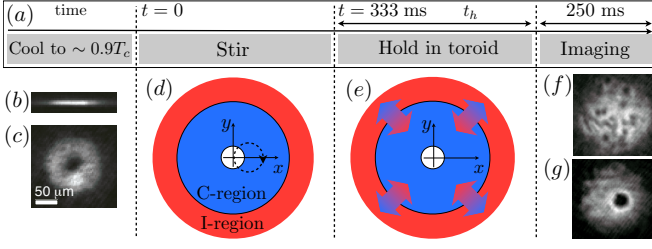


FIG. 1. Schematic of the experimental sequence and simulation parameters. (a) The initial state consists of a trapped Bose gas at  $T \sim 0.9T_c$  in a cylindrically-symmetric harmonic trap augmented with an optically induced Gaussian obstacle potential. The potential is constant in the  $z$  direction and coincident with the symmetry axis of the harmonic trap. In-situ absorption images of the experimental atom density are shown in the transverse (b) and axial (c) directions. (d) The center of the harmonic trap is induced to complete a single revolution around the  $z$ -axis. The obstacle beam executes one circular orbit centered at  $(\bar{x}(t), \bar{y}(t)) = r_0(1 - \cos \kappa t, \sin \kappa t)$ , with  $r_0 = 2.875 \mu\text{m}$ ,  $\kappa = 6\pi \text{ s}^{-1}$ . This is modeled in the frame of the obstacle beam, with an incoherent (I-) region coupled to a coherent (C-) region described with the SPGPE (shown schematically, see text). (e) The dissipation is a significant effect for long time-scales (during the experimental hold). Absorption images after significant hold times show either (f) many vortex cores after an additional radial expansion stage, or (g) a large density minimum corresponding to a persistent current (without radial expansion).

sipative Bose-gas dynamics at high-temperature, provided the incoherent field is not significantly disturbed.

In our c-field description the truncated-Wigner field is expanded on a basis of harmonic oscillator eigenstates. The modes of the system are divided into two distinct regions: the *coherent region* (C) consisting of modes with energy less than a specified cutoff ( $\epsilon_{\text{cut}}$ ), and the *incoherent region* (I) which contains the remaining high energy, quasi-equilibrium states. The I-region acts as a thermal reservoir for the C-region, and is assumed to be in thermal equilibrium at a temperature  $T$  and chemical potential  $\mu$  and is described by a semiclassical Bose-Einstein distribution. The C-region is treated using the truncated Wigner method, where accounting for interactions between the C- and I-regions leads to a stochastic differential equation for the C-region dynamics. The equation of motion is [24]

$$d\psi_{\mathbf{C}}(\mathbf{r}, t) = \mathcal{P}_{\mathbf{C}} \left\{ -\frac{i}{\hbar} L_{\mathbf{C}} \psi_{\mathbf{C}}(\mathbf{r}, t) dt + \frac{\gamma}{\hbar} (\mu - L_{\mathbf{C}}) \psi_{\mathbf{C}}(\mathbf{r}, t) dt + dW(\mathbf{r}, t) \right\}, \quad (1)$$

where the projection operator  $\mathcal{P}_{\mathbf{C}}$  implements the energy cutoff in the spectral basis, and the complex Gaussian noise satisfies  $\langle dW(\mathbf{r}, t) dW(\mathbf{r}', t) \rangle = 0$ ,  $\langle dW^*(\mathbf{r}, t) dW(\mathbf{r}', t) \rangle = (2\gamma k_B T / \hbar) \delta_{\mathbf{C}}(\mathbf{r}, \mathbf{r}') dt$ , where  $\delta_{\mathbf{C}}(\mathbf{r}, \mathbf{r}') = \sum_{n \in \mathbf{C}} \phi_n(\mathbf{r}) \phi_n^*(\mathbf{r}')$  is a delta-function in C.  $L_{\mathbf{C}}$  is the Hamiltonian evolution operator for the C-region  $L_{\mathbf{C}} \psi_{\mathbf{C}} \equiv (H_{\text{sp}} + g|\psi_{\mathbf{C}}|^2) \psi_{\mathbf{C}}$ , where the single-particle Hamiltonian is  $H_{\text{sp}} = -\hbar^2 \nabla^2 / 2m + V(\mathbf{r}, t)$ ,  $g = 4\pi \hbar^2 a / m$  characterizes the strength of the atomic interaction, and  $a$  is the s-wave scattering length.

The first term of the SPGPE (1) describes Gross-Pitaevskii evolution of the C-region, while the second and third terms account the growth of the C-region from scattering of two I-region atoms, and the corresponding time reversed process. Experiments are most commonly described by the system temperature and total atom number  $N_T$ . In the SPGPE implementation, the choice of  $\mu(T, N_T)$  controls the total atom number  $N_T$ , while the choice of  $\epsilon_{\text{cut}}(T, N_T)$  dictates the occupation at the cutoff which must be of order unity for the classical field description of the C-region to be valid [3]. A Hartree-Fock method can be used to accurately estimate SPGPE parameters for harmonically trapped systems close to equilibrium [8]. The growth rate  $\gamma$  can be calculated for near equilibrium situations where the incoherent region is well described by an ideal semiclassical Bose-Einstein distribution, where it takes the form [24]

$$\gamma(T, \mu, \epsilon_{\text{cut}}) = \gamma_0 \sum_{k=1}^{\infty} \frac{e^{\beta \mu(k+1)}}{e^{2\beta \epsilon_{\text{cut}} k}} \Phi \left[ \frac{e^{\beta \mu}}{e^{\beta \epsilon_{\text{cut}}}}, 1, k \right]^2, \quad (2)$$

where  $\Phi[u, v, w]$  is the Lerch transcendent and the dimensionless rate constant is  $\gamma_0 = 8a^2 / \lambda_{dB}^2$  for de Broglie wavelength  $\lambda_{dB} = \sqrt{2\pi \hbar^2 / mk_B T}$ . This explicit calculation of  $\gamma$  means all SPGPE parameters are found in a physically consistent manner prior to simulation, giving a first-principles treatment of damping with no fitted parameters.

We describe the toroidal system using a harmonic-Gaussian external potential  $V(\mathbf{r}, t) = V_{HO}(\mathbf{r}) + V_G(\mathbf{r}, t)$ , where  $V_{HO}(\mathbf{r}) = \frac{m}{2} [\omega_r^2(x^2 + y^2) + \omega_z^2 z^2]$  is the harmonic oscillator potential, and the time dependent Gaussian potential is given by  $V_G(\mathbf{r}, t) = V_0 \exp[-[(x - \bar{x}(t))^2 + (y - \bar{y}(t))^2] / \sigma_0^2]$ . To match the persistent current formation experiment we have  $(\omega_r, \omega_z) = 2\pi \times (8, 90) \text{ Hz}$ ,  $\sigma_0 = 23 \mu\text{m} / \sqrt{2}$ , and  $V_0 = 58 \hbar \bar{\omega}$ , where  $\bar{\omega} = (\omega_r^2 \omega_z)^{1/3}$ . Note this potential has a minimal effect on the I-region as it is well contained within the C-region, since  $\sigma_0 \ll R_{\text{cut}}$ , where  $R_{\text{cut}} = \sqrt{2\epsilon_{\text{cut}} / m\omega_r^2} = 73 \mu\text{m}$  is the spatial cutoff imposed by  $\epsilon_{\text{cut}}$ . Thus our chosen basis gives a complete representation of the C-region.

To model the persistent current experiment we create an initial equilibrium state by evolving Eq. (1) with parameters  $(T, \mu, \epsilon_{\text{cut}}) = (98 \text{ nK}, 34 \hbar \bar{\omega}, 83 \hbar \bar{\omega})$  with the Gaussian potential at  $(\bar{x}, \bar{y}) = (0, 0)$ . These self consistently determined parameters [8] sample the equilibrium ensemble of the SPGPE, giving  $N_T = 2.6 \times 10^6$  total atoms [25], to match the experimental value. For dynamics Eq. (2) gives  $\gamma(98 \text{ nK}, 34 \hbar \bar{\omega}, 83 \hbar \bar{\omega}) = 8 \times 10^{-4}$  and we model the stir by setting  $(\bar{x}(t), \bar{y}(t)) = r_0(1 - \cos(\kappa t), \sin(\kappa t))$ , to move the Gaussian beam in a single circle of radius  $r_0 = 2.875 \mu\text{m}$ , about the point  $(x, y) = (r_0, 0)$ , with angular frequency  $\kappa = 2\pi / (333 \text{ ms}) = 6\pi \text{ s}^{-1}$  (see Fig. 1). During the post-stir hold period where dissipation is a significant effect [Fig. 1 (e)], there is an additional cooling stage of the experiment [19]. Modeling of this process via a time dependent reservoir revealed no significant modification to the dissipative evolution, and thus the details of cooling are omitted here. Our numerical method is a spectral Galerkin method based on

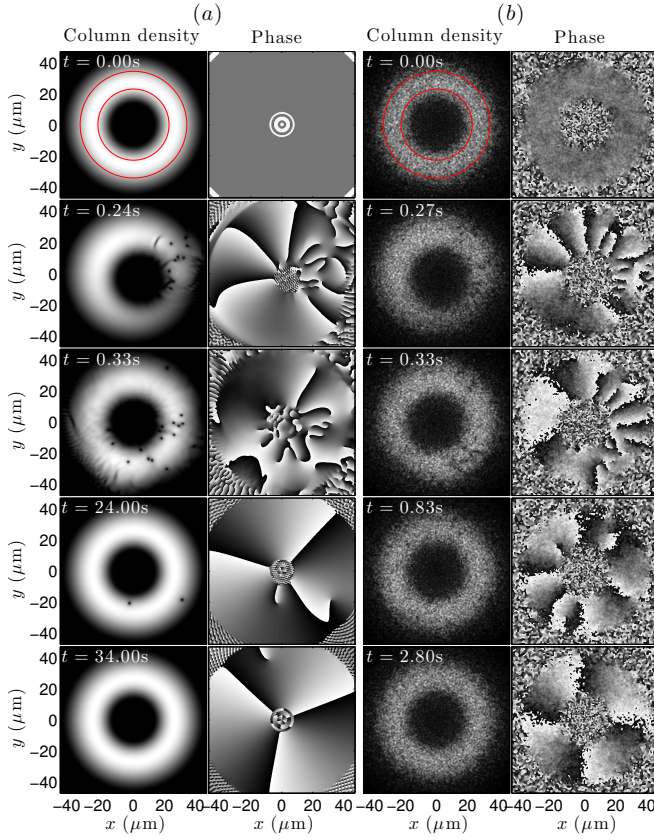


FIG. 2. Column densities and phase slices (through the  $z = 0$  plane) showing the c-field dynamics of modeling the persistent current formation experiment. (a) DPGPE evolution, where dissipation on its own leads to long vortex lifetimes. (b) SPGPE evolution for a single trajectory, where thermal fluctuations greatly increase the vortex decay rate and enhance the size of the persistent current. The red circles at  $t = 0$  s show the boundary of the region within which we count vortices.

Gauss-Hermite quadrature [3, 26]. Due to large particle number, the trap oblateness, and the need for a high energy cutoff, we require  $\sim 10^5$  modes in the C-region, making each trajectory numerically challenging [27]. Our implementation of the DPGPE is identical to that of the SPGPE, without the noise in Eq. (1).

Fig. 2 shows a comparison of individual trajectories of the DPGPE [Fig. 2 (a)] and the SPGPE [Fig. 2 (b)]. The dynamics of both methods are qualitatively similar. Multiple vortices are nucleated during the stirring procedure, which are most easily identified in the phase profile. These vortices evolve in a complicated manner, where they decay through a range of processes: decay to the exterior condensate boundary, internal vortex/antivortex annihilation, or via pinning at the central potential. Finally the system evolves into a stable persistent current with no free vortices in the bulk fluid. However the quantitative differences between the DPGPE and SPGPE are readily apparent from the timescale of the decay of free vortices, and the size of the macroscopic persistent current formed. In Fig. 2 (a) we see the DPGPE requires more than

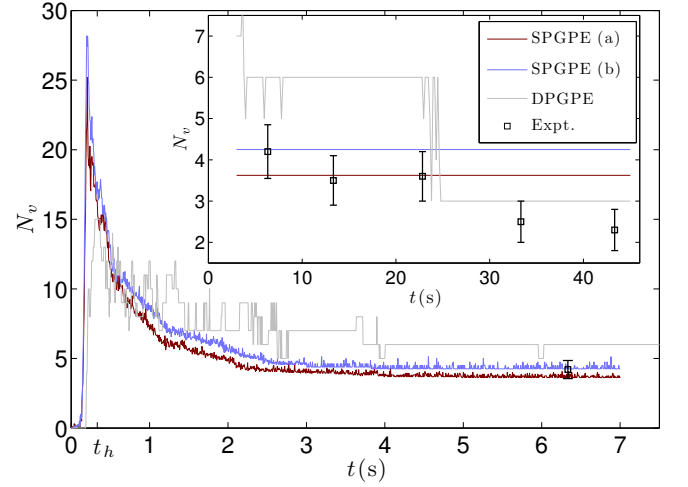


FIG. 3. Average number of vortices  $N_v$  (3) as a function of time  $t$ , where the inset shows the long time dynamics.  $t_h$  corresponds to the end of the 0.333 s stir procedure. The SPGPE ensemble average is shown for  $V_0 = 58\hbar\bar{\omega}$  (SPGPE (a), red), and  $V_0 = 67\hbar\bar{\omega}$  (SPGPE (b), blue), where in both cases a stable persistent current is formed after  $t \sim 3$  s. The DPGPE simulation (gray) develops a stable persistent current after  $t \sim 20$  s. The experimental data is shown by the squares with error bars.

30 s to evolve into a stable persistent current with a circulation of 3 quanta. In contrast, in Fig. 2 (b), SPGPE evolution generates a stable charge-4 persistent current after 2.8 s. The full evolution of one trajectory of the SPGPE is shown in Supplementary Movie S1 [28].

We compare the DPGPE and SPGPE by calculating the number of vortices at a given time in the numerical simulations (in SPGPE we average over 16 trajectories), and comparing this with the number found in the experiment. In counting vortices, we limit our region of detection  $\mathcal{R}$  to radii within  $22.9 \mu\text{m} < \mathcal{R} < 34.4 \mu\text{m}$  centered about the center of the trap, to avoid counting thermal fluctuations. This region is shown in Fig. 2 by the red circles at  $t = 0$  s. Experimentally the vortices were counted after ramping down the Gaussian beam, so this number includes any vortices pinned to the Gaussian beam. Thus we calculate the number of vortices from the numerical simulations via

$$N_v = N_f + N_I \equiv N_f + \left| \frac{m}{\hbar} \oint_{B_I} \mathbf{v}(\mathbf{r}) \cdot d\mathbf{l} \right|, \quad (3)$$

where  $N_f$  is the number free of vortices in the region of detection, and the  $B_I$  is the inner boundary defining the number pinned ( $N_I$ ). Eq. (3) gives the number of vortices in the toroidal condensate including those pinned to the Gaussian potential, thus it can be compared with experimental observations. In Fig. 3 we plot  $N_v$  for the DPGPE simulation (gray curve), and for the SPGPE ensemble average (red curve). We have also included an extra set of SPGPE trajectories (blue curve), where we have used a higher barrier height of  $V_0 = 67\hbar\bar{\omega}$  to account for the experimental uncertainty in this parameter. In this set of simulations we use SPGPE pa-

rameters of  $(T, \mu, \epsilon_{\text{cut}}, \gamma) = (98\text{nK}, 35\hbar\bar{\omega}, 84\hbar\bar{\omega}, 8 \times 10^{-4})$  to give the same atom number and temperature as for the simulations with the lower barrier height of  $V_0 = 58\hbar\bar{\omega}$ . Fig. 3 shows an initial rise in  $N_v$  due to nucleation of vortices from the stir. More vortices are nucleated in the SPGPE simulations. The peak number of vortices occurs at  $t = 0.21$  s in both SPGPE ensemble averages, after which there is a dramatic drop in  $N_v$ . In comparison, the peak number of vortices occurs at  $t = 0.33$  s in the DPGPE, and  $N_v$  decreases more gradually. We compare these calculations with available experimental data (black squares). Both SPGPE calculations agree well with the first experimental data point at  $t = 6.33$  s, lying within the experimental uncertainty. At this stage  $N_v$  has reached a stable value for the SPGPE simulations, where all free vortices have left the condensate and the system is in a stable persistent current. In contrast, there are still many free vortices after  $t = 6.33$  s in the DPGPE simulation.

The quantitative difference at long evolution times is shown in the inset of Fig. 3, where we compare the data of simulations and experiment. Experimentally,  $N_v$  decays due to a loss of pinned vortices caused by a slow drift in the magnetic trap center [19]. This means the drop in  $N_v$  is due to the lack of complete control of the trap, rather than decay of free vortices. This is also supported by experimental column densities where we observe no evidence of free vortices for  $t > 10$  s [29]. Thus the agreement of  $N_v$  (at  $t = 6.33$  s) between the SPGPE calculations and experiment show that the SPGPE accurately predicts the size of the persistent current, and the decay-time of free vortices in the condensate. Free vortices exist in the DPGPE simulation for the first 20 s of evolution, over which time  $N_v$  is never comparable with experiment. After  $t = 22$  s, the DPGPE stabilizes into a charge 3 persistent current. Note that this is smaller than that seen with

the SPGPE, and is only similar to the experimental persistent current for times longer than 20 s.

The vortex detection region is limited by the ability to see free vortices in competition with thermal fluctuations in the SPGPE simulations. Thus the absence of thermal fluctuations in the DPGPE simulation means that  $N_v$  found with our specified  $\mathcal{R}$  is a lower bound. In Fig. 2 (a), we see there are free vortices present at  $t = 24$  s, despite Fig. 3 showing that the system has reached a stable persistent current at this time.

In summary, we have modeled the persistent current experiment of Neely *et al.* [19] using the grand-canonical c-field method. The SPGPE theory of reservoir interactions predicts a persistent current formation time and winding number that closely matches the experiment. Such quantitative accuracy is not provided by the damped GPE, and the regime of significant vortex dissipation in the experiment ( $T \approx 0.9T_c$ ) is well outside the region of validity of generalized mean-field theories. In general, both damping and noise are required to give a quantitative description of dissipation in open quantum systems, and our results demonstrate the central importance of thermal noise in high temperature Bose gas dynamics. We have demonstrated the crucial effect thermal fluctuations have on the physical decay of quantized vortices, and performed an a priori quantitative test of the SPGPE. Our approach provides a general quantitative framework for studying high-temperature dynamics in three-dimensional Bose gases.

SR thanks Victoria University where this work was finished for their hospitality. We are supported by the New Zealand Foundation for Research, Science, and Technology (contracts UOOX0801 and NERF-UOOX0703) (AB), and The University of Otago (SR). The experimental work was supported by the US National Science Foundation.

- 
- [1] I. Bloch, J. Dalibard, and W. Zwerger, *Rev. Mod. Phys.* **80**, 885 (2008).
  - [2] N. P. Proukakis and B. Jackson, *J. Phys. B-At. Mol. Opt.* **41**, 203002 (2008).
  - [3] P. B. Blakie *et al.*, *Adv. in Phys.* **57**, 363 (2008).
  - [4] E. Zaremba, T. Nikuni, and A. Griffin, *J. Low Temp. Phys.* **116**, 277 (1999).
  - [5] D. Dagnino, N. Barberan, M. Lewenstein, and J. Dalibard, *Nat. Phys.* **5**, 431 (2009).
  - [6] M. J. Davis and P. B. Blakie, *Phys. Rev. Lett.* **96**, 060404 (2006).
  - [7] S. A. Morgan, M. Rusch, D. A. W. Hutchinson, and K. Burnett, *Phys. Rev. Lett.* **91**, 250403 (2003).
  - [8] B. Jackson and E. Zaremba, *Phys. Rev. Lett.* **88**, 180402 (2002).
  - [9] S. J. Rooney, A. S. Bradley, and P. B. Blakie, *Phys. Rev. A* **81**, 023630 (2010).
  - [10] M. R. Matthews *et al.*, *Phys. Rev. Lett.* **83**, 2498 (1999).
  - [11] B. P. Anderson, *J. Low Temp. Phys.* **161**, 574 (2010).
  - [12] L. M. Pismen, *Vortices in Nonlinear Fields*, 1st ed. (Oxford University Press, New York, 1999).
  - [13] P. C. Haljan, I. Coddington, P. Engels, and E. A. Cornell, *Phys. Rev. Lett.* **87**, 210403 (2001).
  - [14] K. W. Madison, F. Chevy, W. Wohlleben, and J. Dalibard, *Phys. Rev. Lett.* **84**, 806 (2000).
  - [15] B. Jackson, N. P. Proukakis, C. F. Barenghi, and E. Zaremba, *Phys. Rev. A* **79**, 053615 (2009).
  - [16] C. W. Gardiner and M. J. Davis, *J. Phys. B* **36**, 4731 (2003).
  - [17] S. J. Rooney, P. B. Blakie, B. P. Anderson, and A. S. Bradley, *Phys. Rev. A* **84**, 023637 (2011).
  - [18] C. N. Weiler *et al.*, *Nature* **455**, 948 (2008).
  - [19] C. Ryu *et al.*, *Phys. Rev. Lett.* **99**, 260401 (2007).
  - [20] T. W. Neely *et al.*, Characteristics of Two-Dimensional Quantum Turbulence in a Compressible Superfluid, arXiv:1204.1102, 2012.
  - [21] S. Choi, S. A. Morgan, and K. Burnett, *Phys. Rev. A* **57**, 4057 (1998).
  - [22] A. A. Penckwitt, R. J. Ballagh, and C. W. Gardiner, *Phys. Rev. Lett.* **89**, 260402 (2002).
  - [23] M. Tsubota, K. Kasamatsu, and M. Ueda, *Phys. Rev. A* **65**, 023603 (2002).
  - [24] C. W. Gardiner, J. R. Anglin, and T. I. A. Fudge, *J. Phys. B: At. Mol. Opt. Phys.* **35**, 1555 (2002).
  - [25] A. S. Bradley, C. W. Gardiner, and M. J. Davis, *Phys. Rev. A* **77**, 033616 (2008).
  - [26] The details of a self-consistent method of accounting for the above-cutoff atom number are given in Ref. [8].

- [26] P. B. Blakie, Phys. Rev. E **78**, 026704 (2008).
- [27] Our numerical method implements the energy cutoff exactly but scales poorly with basis size [26]. Each trajectory of the SPGPE takes  $\sim 50$  days of wall clock time to propagate for 7 s of system evolution, on the University of Otago Vulcan computing cluster with 2.66 GHz CPUs.
- [28] See Supplemental Material at [URL will be inserted by publisher] for Movie S1.
- [29] T. W. Neely, Ph.D. thesis, University of Arizona, Tucson Arizona, USA, 2010.